Sporadic sodium layer: A possible tracer for the conjunction between the upper and lower atmospheres

Shican Qiu[1,2,3], Ning Wang[1,4,5], Willie Soon[6], Gaopeng Lu[2], Mingjiao Jia[2,3], Xianghui Xue[2,3], Tao Li[2,3],

Xiankang Dou[2,3]

[1]Department of Geophysics, College of the Geology Engineering and Geomatics, Chang'an University, Xi'an, 710054, China

[2]Key Laboratory of Geospace Environment, Chinese Academy of Sciences, University of Science & Technology of China, Hefei, Anhui, 230026, China

[3]Mengcheng National Geophysical Observatory, School of Earth and Space Sciences, University of Science and Technology of China, Hefei, Anhui, 230026, China

[4]Gravity & Magnetic Institute of Chang'an University, Xi'an, 710054, China

[5]Key Laboratory of Western China's Mineral Resources and Geological Engineering, China Ministry of Education, Xi'an, 710054, China

[6]Center for Environmental Research and Earth Sciences (CERES), Salem, Massachusetts, 01970, USA

Correspondence to: Shican Qiu (*scq@ustc.edu.cn*) *and Xiankang Dou (dou@ustc.edu.cn*)

Abstract. In this research, we reveal the inter-connection between lightning strokes, reversal of the electric field, ionospheric disturbances, and a sodium layer (Na_S), based on the joint observations by two lidars, an ionosonde, an atmospheric electric mill, a fluxgate magnetometer, and the World Wide Lightning Location Network (WWLLN). Our results suggest that lightning strokes would probably have an influence on the ionosphere and thus affecting the occurrence of Na_S, with the overturning of electric field playing an important role. Statistical results reveal that the sporadic E layers (E_S) could hardly be formed or maintained when the atmospheric electric field turns upward. A conjunction between the lower and upper atmospheres could be established by these inter-connected phenomena, and the key processes could be suggested as follows: lightning strokes→overturning of electric field→depletion of E_S/generation of Na_S.

Keywords: sporadic sodium layers, sporadic E layers, atmospheric circuit, lightning stroke, electric field

1 Introduction

The upper mesosphere-lower thermosphere (MLT) region, is the junction for momentum and energy exchanges between the Earth's low atmosphere and outer space. However, on account of the limitations of detection methods, this region remains the least known part of our planet's atmosphere (Wang, 2010). Fortunately, the metal layers (especially the sodium layer), which located between about 80 ~ 110 km, could possibly act as a window to detect the MLT parameters by means of fluorescence resonance lidars (Gardner et al., 1986; Gong et al., 2002; Gong et al., 1997). With an active chemical property and high abundance of sodium atoms, the sodium layer has been widely observed and studied all over the world (Marsh et al., 2013; Collins et al., 2002; Plane, 2003; Plane et al., 1999). The sporadic sodium layer (SSL or Na_S), with the neutral sodium density that could double within several minutes, is the most fantastic phenomenon observed from the sodium layer. Since first reported in 1978 (Clemesha et al., 1978), many mechanisms, involving meteor injection (Clemesha et al., 1980), dust reservoir (von Zahn et al., 1987), recombination of ions and electrons in sporadic E layer (E_S) (Cox and Plane, 1998), and high temperature theory (Zhou et al., 1993), have all been proposed. Because the Na_S is suggested to have a connection to so many atmospheric parameters, the metric or phenomenon could be appropriate in acting as a tracer for studying inter-connection between the middle and upper atmospheres. Up to now, a large number of observations report a diversity of the Na_S features, but the exact mechanism for Na_S is probably still uncertain (Collins et al., 2002; Cox et al., 1993; Daire et al., 2002; Gardner et al., 1995; Qiu et al., 2015; Zhou and Mathews, 1995; Zhou et al., 1993).

Among all the proposed mechanisms, the E_S theory is supported by abundant observations and results from numerical simulations (Cox and Plane, 1998; Daire et al., 2002; Dou et al., 2009; Dou et al., 2010; Gardner et al., 1993; Gong et al., 2002; Kane et al., 2001; Kane et al., 1993; Kane et al., 1991; Kirkwood and Nilsson, 2000; Kwon et al., 1988; Mathews et al., 1993; Miyagawa et al., 1999; Nagasawa and Abo, 1995; Nesse et al., 2008; Shibata et al., 2006; Williams et al., 2006). The key process of E_S theory is the recombination of ions and electrons in the E_S layer while descending to lower altitudes (Cox and Plane, 1998; Daire et al., 2002). The E_S layer is mainly influenced by the vertical wind shear (Abdu et al., 2003; Clemesha et al., 1998; Haldoupis et al., 2004; Mathews, 1998; Šauli and Bourdillon, 2008; Wakabayashi and Ono, 2005), the geomagnetic field (Resende et al., 2013; Resende and Denardini, 2012; Zhang et al., 2015; Denardini et al., 2016), and the electric field (Abdu et al., 2003; Damtie et al., 2003; Haldoupis et al., 2004; Kirkwood and Nilsson, 2000; Kirkwood and von Zahn, 1991; Macdougall and Jayachandran, 2005; Matuura et al., 2013; Nygren et al., 2006; Parkinson et al., 1998; Takahashi et al., 2015; Voiculescu et al., 2006; Wakabayashi and Ono, 2005; Wan et al., 2001; Wilkinson et al., 1993). In the Northern Hemisphere, the E_S layer would descend to a lower altitude during southward electric field (Abdu et al., 2003; Damtie et al., 2003; Haldoupis et al., 2004; Kirkwood and Nilsson, 2000; Kirkwood and von Zahn, 1991; Macdougall and Jayachandran, 2005; Nygrén et al., 2006; Parkinson et al., 1998; Takahashi et al., 2015; Voiculescu et al., 2006; Wakabayashi and Ono, 2005; Wan et al., 2001; Wilkinson et al., 1993), and observations in the polar cap suggest the electric field reversal have an influence on the probability of E_S occurrences (Macdougall and Jayachandran, 2005).

On the other hand, the atmospheric electric circuit is a closed loop (Driscoll et al., 1992; Jánský and Pasko, 2014; Lv et al., 2004; Roble and Hays, 1979; Rycroft and Harrison, 2012; Rycroft et al., 2000; Suparta and Fraser, 2012; Tinsley, 2000), like a capacitor with a positive plate (e.g., the ionosphere) and a negative panel (e.g., the ground), and dielectric medium between them (e.g., the neutral atmosphere). Then the global atmospheric electric circuit formed in the capacitor, with the lightning phenomena generating an upward current (with the atmospheric electric field intensity $E<0$) and returning a downward current ($E>0$) under fair weather condition. Nowadays increasing and emerging evidences are pointing to the close link between the upper atmosphere (e.g., the positive plate) and lower atmosphere (e.g., the negative plate) (Harrison et al., 2010; Rycroft, 2006). For example, thunderstorm occurring in the lower atmosphere is suggested to have a direct impact on the E_S layer based on recent observational results (Bortnik et al., 2006; Christos, 2018; Cummer et al., 2009; Curtius et al., 2006; Davis and Johnson, 2005; Davis and Lo, 2008; England et al., 2006; Fukunishi et al., 1996; Girish and Eapen, 2008; Haldoupis et al., 2012; Immel et al., 2013; Kumar et al., 2009; Kuo and Lee, 2015; Lay et al., 2015; Mangla et al., 2016; Maruyama, 2006; Pasko et al., 2002; Rodger et al., 2001; Rycroft, 2006; Sátori et al., 2013; Sentman and Wescott, 1995; Shao et al., 2013; Sharma et al., 2004; Su et al., 2003; Surkov et al., 2006; Yu et al., 2015) or even the sodium layer (Yu et al., 2017). The possible carriers or phenomena connecting the thunderstorm to the upper atmosphere are suggested to be atmospheric tides (England et al., 2006; Haldoupis et al., 2004; Immel et al., 2013), planetary waves (Lv et al., 2004), gravity waves (Davis and Johnson, 2005; Kumar et al., 2009; Lay et al., 2015; Shao et al., 2013), transient luminous event (TLEs) (Cummer et al., 2009; Fukunishi et al., 1996; Haldoupis et al., 2012; Pasko, 2008; Pasko et al., 2002; Sentman and Wescott, 1995; Sharma et al., 2004; Su et al., 2003), the solar activity (Zhang et al., 2020), and also the electric fields (Bortnik et al., 2006; Davis and Johnson, 2005; Davis and Lo, 2008; Immel et al., 2013; Kuo and Lee, 2015; Maruyama, 2006; Rycroft, 2006; Sátori et al., 2013; Shao et al., 2013).

In this research, we apply five joint observations for our case studies and statistical works: (1) Two lidars at Hefei (31.8ºN, 117.2ºE), providing observations of sodium density, mesopause temperature and zonal wind; (2) An ionosonde in Wuhan (30.5°N，114.6°E), detecting the E_S and ionospheric echoes in different modes; (3) An atmospheric electric mill (30.5ºN, 114.5ºE), giving simultaneous electric field variations; (4) A fluxgate magnetometer (30.5ºN, 114.5ºE), probing the H, D, and Z magnetic field components; and (5) The World Wide Lightning Location Network (WWLLN), observing the location and power of a lightning stroke. The purpose of this study is to examine the possibility of Na_S acting as a practical robust tracer for the conjunction between the upper and lower atmospheres. Our results suggest that lightning strokes may have an influence on the lower ionosphere leading to the occurrence of Na_S, with the atmospheric electric field probably playing an important role.

2 Observations and results

2.1 An Na_S event during the overturning of electric field

A sporadic sodium layer is detected on the night of June 3rd, 2013, by both the USTC sodium lidar (Dou et al., 2009) and the nearby Temperature/Wind (T/W) lidar (Li et al., 2012) (in Fig. 1a and 1b, the same Na_S event detected with different resolutions). The peak density of Nas detected by the wideband lidar is more than 12000 cm^{-3}, while the peak density observed by narrowband lidar is about 5000 cm^{-3}. The discrepancy of peak densities may come from the wideband lidar. Fig. 1(a) shows the wideband lidar system operated poorly after the midnight. For the sodium lidar, the inversion formula for the sodium number density *N* at an altitude of *z* is given as follows:

$$N = \frac{\sigma_R n_a(z_0)}{\sigma_{N_a}} \cdot \frac{(P(z)-P_B)z^2}{(P(z_0)-P_B)z_0^2}, \quad (1)$$

where σ_R is the Rayleigh backscatter cross section; $n_a(z_0)$ is the atmosphere density at a reference altitude, given by atmospheric model; σ_{N_a} is the effective sodium backscatter cross section; $P(z)$ is the number of photons detected in the range interval (z-Δz/2, z+Δz/2); P_B is the expected photon count per range bin due to background signal and dark counts, calculated through the averaged background signal above 130 km; and, $P(z_0)$ is the Rayleigh photon count at 30 km altitude, estimated by averaging the measured photon count over a 5-km range interval centered at 30 km (Gardner et al., 1986; Xue, 2007). The averaged photon count $P(z_0)$ at 30 km is $P(z_0) = 106$ (smaller than that on normal days), and the expected photon count P_B at 130 km equals to 18 (larger than that on normal days). Since the error term is inversely proportional to the absolute value of $P(z_0) - P_B$, a much smaller $|P(z_0) - P_B|$ would cause an increase in the deduced sodium number density *N*.

This Na_S event occurs much higher above the centroid height of sodium layer (normally at about 92 km). Both Fig. 1a and 1b show the sodium density begins to increase at about 13:20 UT, while the largest intensity of sodium enhancement occurs from about 14:20 UT, with a peak density on 97.75 km at 14:40 UT. The simultaneous temperature observation by the T/W lidar reveals this Na_S occurs in a cold region (Fig. 1c), so the high temperature mechanism appears to be inapplicable for this event.

On the other hand, the zonal wind exhibits a suitable wind shear for creating those sporadic E layers, with a westward wind above and an eastward wind below (Fig. 1d). The E_S layer is predicted to form around the border of the wind shear. Observations by the ionosonde at Wuhan indeed show active sporadic E layers on that day (Fig. 2a and b). The E_S series keep travelling/propagating downward starting around 6:30 UT, and then disappear at last while the Na_S occurs coincidently on about 13:20 UT. So this Na_S is better explained by the E_S mechanism, in accord with our previous study which shows that a Na_S higher than 96 km tends to be controlled by the E_S mechanism (Qiu et al., 2016). Although the content of sodium ions in E_S layers seemed to have insufficient concentration (von Zahn et al., 1989), it has also been proposed that the ions could be concentrated by the wind shear effectively (Clemesha et al., 1999; Cox and Plane, 1998; Nesse et al., 2008). On the other hand, laboratory results show that the ligand complexes of $Na^+ \cdot X$ would form and thus speed up the recombination of ions in

the mesopause condition (Collins et al., 2002; Cox and Plane, 1998; Daire et al., 2002). The calculated reaction rate suggests the formation of cluster ions is enhanced at lower temperatures, in accordance with the cold region observed in Fig. 1c where the sporadic sodium layer occurs.

More details about the atmospheric parameters are shown in Fig. 3. The time series of sodium density on the peak height display a sharp enhancement from 14:20 UT (marked by the vertical red dashed line in Fig. 3a). The atmospheric electric field detected by the mill exhibits an overturning at around 14:20 UT, alternating from downward direction to upward (Fig. 3b). It can be clearly observed that the enhancement of sodium density occurs coincidentally with the overturning of electric field, as highlighted by the vertical red dashed line in Fig. 3. A nearby fluxgate magnetometer provides the horizontal magnetic field *H* (nT) (Fig. 3c), showing disturbances at 14:15 UT. The total magnetic intensity *B* could be deduced by the *H*, *Z*, and *D* components ($B = \sqrt{H^2 + D^2 + Z^2}$) from fluxgate magnetometer observations (the calculated values are plotted in Fig. 3d).

It is worth noting that the overturning of atmospheric electric field discussed here is theoretically rough, since the electric field at the lower ionosphere will be modulated as well (e.g., with a value of several mV/m [Seyler et al., 2004)]). Nevertheless, model simulations from the electrodynamics show that the upward electric field in upper atmosphere is proportional to the source current in the troposphere (Driscoll et al., 1992), and that the upward current would continue transmitting to the heights of 100~130 km of the dynamo region where E_S occurs most frequently (Rycroft et al., 2012). The model, based on rocket observations, shows that the atmospheric electric field has a similar scale and the same polarity from the ground to the altitude of ionosphere (Abdu et al., 2003). Thus, the electric field detected by a ground-based mill could reasonably be a reflection of the actual situation in the lower ionosphere, at least for the trends of variations.

2.2 Statistical results of the E_S and overturning of electric field

A statistical correlation between the overturning of electric field and E_S variations is summarized in Table 1. The foE_S values refers to the Critical Frequency, at which the reflection starts while the radio frequency equals the plasma frequency ($foE_S = \omega_{pe} = \left(\frac{n_e e^2}{m_e \varepsilon_0}\right)^{\frac{1}{2}} \approx 9\sqrt{10^{-6} n_e}$, with foE_S in MHz and n_e in cm^{-3}) (Bittencourt, 2004). From 2012 to 2014, in the summer season (from May to August, when the E_S layers occur frequently), there are 242 days with effective observations of E_S and electric field with the overturning feature. Among all the cases, for about 155/242 days the foE_S get interrupted during the overturning of electric field, while the foE_S decreases on 39/242 days. In comparison, foE_S appears only for 6/242 days, and increases for 26/242 days. Another 28/242 days show no distinguishing features of the E_S during an overturning of the electric field. These ratios are overlapped, since sometimes there are more than one overturning on a single day. Thus in general, these results suggest that E_S could hardly be formed for upward electric field situations and that indeed the overturning of electric field causes a depletion of E_S. This statistical result may also give an implication that the electric field variations detected by ground based mill have a feasible link with the lower ionosphere. It is worth mentioning that there is

indeed no one-to-one correspondence between the electric field overturning and E_S depletion, since the E_S is also influenced by other key parameters and phenomena including wind shears, tides and gravity waves. Sometimes the overturnings recover quickly, without sufficient time for producing an obvious effect on E_S. Therefore a deeper analysis will be needed in future statistical studies.

3 Discussions

3.1 Possible influences by the atmospheric electric circuit

The atmospheric electric circuit is formed by the ionosphere and ground surface with the dielectric medium (e.g., the neutral atmosphere) sandwiched between them (Driscoll et al., 1992; Harrison, 2020; Jánský and Pasko, 2014; Lv et al., 2004; Roble and Hays, 1979; Rycroft and Harrison, 2012; Rycroft et al., 2000; Rycroft et al., 2012; Rycroft et al., 2007; Suparta and Fraser, 2012; Tinsley, 2000). The lightning phenomena and thunderstorms, acting as the electric generator for the circuit, drive an upward current to the ionosphere. In fair weather regime, the electric field directs downward to the earth surface ($E > 0$), making a closed global electric circuit (see Fig. A1 in Appendix). The electric field could vary through two distinct ways as follows: The first one is the changing magnetic field explained by the Faraday's law (e.g. , $\nabla \times \vec{E} = -\frac{\partial \vec{B}}{\partial t}$). However, observations by the fluxgate magnetometer show that there is just a small disturbance of magnetic field during the overturning of electric field. The other way is the electrostatic induction following the Coulomb's law ($\vec{E} = \frac{1}{4\pi\varepsilon_0}\frac{Q}{r^2}\hat{r}$). The connection between the lightning stroke and the overturning of electric field could be explained by a classic thunderstorm charge model through the electric imaging method based on the Coulomb's law (i.e., this model could be supported by a classic electrodynamics textbook written by D.J. Griffiths, 1999). A typical thundercloud (e.g., pairs of (Q_1, —Q_2) or (—Q_3, Q_4) in Fig. A1), with a dipole of positive charge located above a negative charge part, would produce an upward electric field toward the ionosphere (see more details in Appendix A).

According to the observations from WWLLN, we find two regions (red ovals A and B in Fig. 4) with heavy lightning activities during the period of the Na_S. Before the Na_S occurrences, there were only a few powerful lightnings detected within about (25.1°N ~ 35.8°N) and (113.8°E ~ 118.1°E) during the period of 12 UT to 13:15 UT (just one strong stroke with a power of 43720.25 kW happening on 12:17 UT, at 25.7229°N and 117.3955°E). The continuous strongest lightnings with a power larger than 10^4 kW occur from 13:19 UT to 15:43 UT, mainly concentrating in two areas centered around (35.8°N, 118.1°E) and (25.1°N, 113.8°E). After 15:45 UT, no strong strokes were detected again within this area. Thus, the pairs of (Q_1, —Q_2) and (—Q_3, Q_4) could be referred to the lightning area of part A and B in Fig. 4. Since thunderstorms could trigger the breakdown process within a rather large area (Leblanc et al., 2008) and influenced the ionosphere with around more than 800 km range horizontally away from the lightning center (Johnson and Davis, 2006; Johnson et al., 1999), the whole area above might undergo a breakdown easily around $Q_1 \sim Q_4$ (e.g., the whole shadow zone in Fig. 4, involving the two strongest lightning areas and the two observing stations).

In previous studies, lightning strokes in lower atmosphere were reported to cause a reduction of electrons of the ionosphere (Shao et al., 2013), and in reverse an enhancement of sodium density in the metal layer (Yu et al., 2017). Those two scenarios are in accord with our current results presented above, with a depletion of E_S and a consequential occurrence of Na_S. Although such an idea/picture has been proposed long time ago (Griffiths, 1999), this is the first time that one can apply the imaging method for observing thunderstorms to explain the link between upper and lower atmospheres through an overturning of upward electric field.

Furthermore, the results from different channels of Wuhan ionosonde exhibit extraordinary echoes in different modes during the lightning period (Fig. 5a to 5l). (a) ~ (c): From 13:15 UT to 13:45 UT, the echoes gradually increase. Note that the powerful lightning period begins on 13:15 UT as well, with the sodium density enhancement and the E_S depletion occurring on about 13:20 UT. (d) ~ (g): Most intense echo signals occur during 14:00 UT to 14:45 UT, while the largest intensity of sodium enhancement begins at 14:20 UT and the sodium density peaks at 14:40 UT. The overturning of electric field also occurs at 14:20 UT. (h) ~ (j): From 15:00 UT to 15:30 UT, the signals weaken gradually; (k) ~ (l): The echoes vanish after 15:45 UT. Afterwards, no strong stroke detected again in the discussed area. Meanwhile, the ionospheric echoes diminish after 15:45 UT, and the overturning of electric field also recovers at about 15:30 UT. Thus, in this case the ionospheric echoes and the lightning activities exhibit an obvious synchronous behavior.

3.2 Possible mechanism for Na_S

Usually, the mid-latitude E_S layers would be brought down gradually by tidal fluctuations (Mathews, 1998). The E_S theory predicts that when a series of E_S layers descend below 100 km, they will be depleted through the recombination of ions and electrons (Cox and Plane, 1998). Since the recombination of $Na^+ + e^- \rightarrow Na + h\nu$ is inefficient to generate Na_S, Na^+ is believed to first form a ligand $Na^+ \cdot N_2$ through the recombination reaction:

$$Na^+ + N_2 + M \rightarrow Na^+ \cdot N_2 + M, \quad (2)$$

with a rate coefficient of $k_1 = 4.8 \times 10^{-30}(T/200)^{-2.2}$ cm^6 $molecule^{-2}$ s^{-1} (Cox and Plane, 1998). $Na^+ \cdot N_2$ can either switch with CO_2 (which will undergo dissociative electron recombination to form Na), or O (which reforms Na^+) (Cox and Plane, 1998). Thus the key factor of E_S mechanism depends on the ratio of [O]/ [CO_2]: Recombination of $Na^+ \cdot CO_2$ and e^- will increase rapidly as [O]/ [CO_2] decreases below a value of 100 (Cox and Plane, 1998). Then the sodium atoms could be formed directly from the following chemical reaction:

$$Na^+ \cdot CO_2 + e^- \rightarrow Na + CO_2. \quad (3)\ \text{(Cox and Plane, 1998)}$$

The chemical reaction rate (v) for this second-order reaction could be calculated using the following equation:

$$v = k[Na^+ \cdot CO_2]N_e, \quad (4)$$

The reaction rate coefficient k_2 for the chemical reaction (3) is experimentally measured to be:

$$k_2 = 1 \times 10^{-6}\sqrt{\frac{200}{T}}\ (cm^6\,molecule^{-2}\,s^{-1}) \quad (5)$$

(Collins et al., 2002; Cox and Plane, 1998; Daire et al., 2002), and the electron density N_e could be calculated using the following equation:

$$N_e = 1.24 \times 10^4 f o E_S^2 (cm^{-3}) \quad (6) \text{ (Bittencourt, 2004).}$$

Overall, this E_S mechanism is most widely accepted, if we neglect k_1 for reaction (2) as being too small with an order of 10^{-30}. A possible adaptation is to assume a plenty quantity of pre-existing $Na^+ \cdot N_2$ or $Na^+ \cdot CO_2$ in the sodium layer, and then the E_S just needs to provide enough additional electrons. Figure 2(b) shows E_S descending near 100 km at about 13:20 UT. Then the E_S depletes, and a moderate enhancement of Na occurs from 13:30 UT to 14:00 UT (shown in Figure 1(a) and 3(a)). This increase in sodium density exhibits no obvious peak, which could probably be in accord with a normally descending E_S governed by tides. In comparison, the peak profile of the Na_S shows intense enhancement and sharp peak, indicating a distinct mechanism.

On the other hand, a link between the reverse electric field and E_S variations could be established through the acceleration of electrons. Normally, positive particles will move along the direction of electric field, and negative particles do opposite (Griffith and College, 1999). Since metal ions are much heavier than electrons, the ions would drag electrons to move/drift together, which is called the bipolar diffusion (Griffiths, 1999). In the initial stage, ions and electrons descend gradually under the southward electric field. In a partially ionized plasma, the characteristic frequencies for ions and electrons are associated with the collisions of the plasma particles with stationary neutrals (e.g., the electron–neutral collision frequency ν_{en} and the ion–neutral collision frequency ν_{in}). The collision frequency ν_{sn} for scattering of the plasma species s by the neutrals is

$$\nu_{sn} = n_n \sigma_s^n V_{Ts}\,, \quad (7) \text{ (Shukla and Mamun, 2002)}$$

where n_n is the neutral number density,

σ_s^n is the scattering cross section (which is typically of the order of 5×10^{-15} cm^2 and depends weakly on the temperature Ts),

and $V_{Ts} = (k_B T_s / m_s)^{1/2}$ is the thermal speed of the species s.

So the relaxation times $\tau = \frac{1}{\nu}$ for ions and electrons are different in a partially ionized plasma, and electrons would respond much faster than the heavier sodium ions do (since $m_i \gg m_e$). At the moment when the electric field reverses, electrons will be rapidly accelerated by the northward electric field, and ions would be regarded as essentially remaining northward or unchanged. If we could possibly assume that $Na^+ \cdot CO_2$ is always excessive (as we see from estimates below it just needs to be a number density of 100 cm^{-3}, but regrettably there is no direct measurements and detections up till now), we only need to consider the amount of electrons. When the reactant concentration for R(3) is increased (e.g., when a concentrated electron layer accelerated downward below 100 km), this reaction will shift to the right side of R(3). To calculate the chemical reaction rate, we assumed a pre-existing concentration of 100 cm^{-3} for $[Na^+ \cdot CO_2]$, and used the observed value of 3.1 MHz for foE_S (means $N_e = 1.2 \times 10^5$ cm^{-3}), and 170 K for T. The calculated rate is $v = 13$ cm^{-3}s^{-1}, in accord with the required source strength of sodium atoms of 3 sodium atoms cm^{-3}s^{-1} for the formation of Na_S (Cox et al., 1993). If we deduct some

influences by eddy diffusion and loss of sodium atoms, this chemical rate can generate a Na_S within several minutes. Thus, no matter how many Na^+ ions are in E_S, the electrons in E_S are always sufficient to produce Na_S. Perhaps that is the reason why we often observe even a very weak E_S is accompanied by Na_S (Dou et. al., 2010).

Based on the above results, a possible mechanism for Na_S could be suggested by the following four steps: (1) Strong lightning strokes produce an upward atmospheric electric field toward the ionosphere; (2) The reverse of electric field would accelerate the electrons in E_S layer to descend rapidly; (3) The concentrated electrons meet with pre-existing sodium reservoir of $Na^+ \cdot CO_2$ below 100 km, making a faster recombination through the most efficient reaction of $Na^+ \cdot CO_2 + e^- \rightarrow Na + CO_2$; (4) The depleted E_S layers generate the formation of Na_S. Thus, we propose that there would probably be a connection between the lightning strokes, overturning of the electric field, ionospheric disturbances, and also the Na_S. A link between the lower and upper atmospheres could be established by carefully studying and examining these phenomena. However, it is worth noting that the key processes during step (2) and (3) remained still quite uncertain. A more in-depth modelling study concerning both plasma and neutral molecules is needed in the future.

4 Conclusions

In this research, we study the conjunction between the lower and upper atmospheres, through the phenomena and processes of lightning strokes, overturning of the atmospheric electric field, ionospheric disturbance, plasma drift velocity reversal, and the formation and dissipation of sporadic sodium layer. The main findings of our results are summarized as follows:

1. The Na_S event discussed in the present case study shows a close relationship with E_S activities rather than conforming with the prescriptions from high temperature theory.
2. The atmospheric electric field exhibits an overturning, opposite to the fair weather downward field in circuit, in coincident with the depletion of E_S and the consequent production of Na_S.
3. A statistical analysis shows that the E_S could hardly be formed or maintained when the atmospheric electric field is directed upward.
4. A typical thunderstorm with a positive charge located above a negative charge layer, is shown to produce an upward electric field toward the ionosphere. Two regions with heavy lightning activities nearby are found during the overturning of the atmospheric electric field.
5. Observations by the ionosonde exhibit extraordinary echoes during the lightning period and the temporal property of the echoes behaved synchronously with lightning activities.

Our results support a physical connection between the lightning strokes, overturning of the electric field, ionospheric disturbances, and also possibly the Na_S phenomenon. A link between the lower and upper atmospheres could be established by the monitoring of Na_S and related phenomena as follows: lightning strokes→overturning of electric field→depletion of E_S/generation of Na_S.

Appendix A: Calculations for the induced upward electric field in the global electric circuit

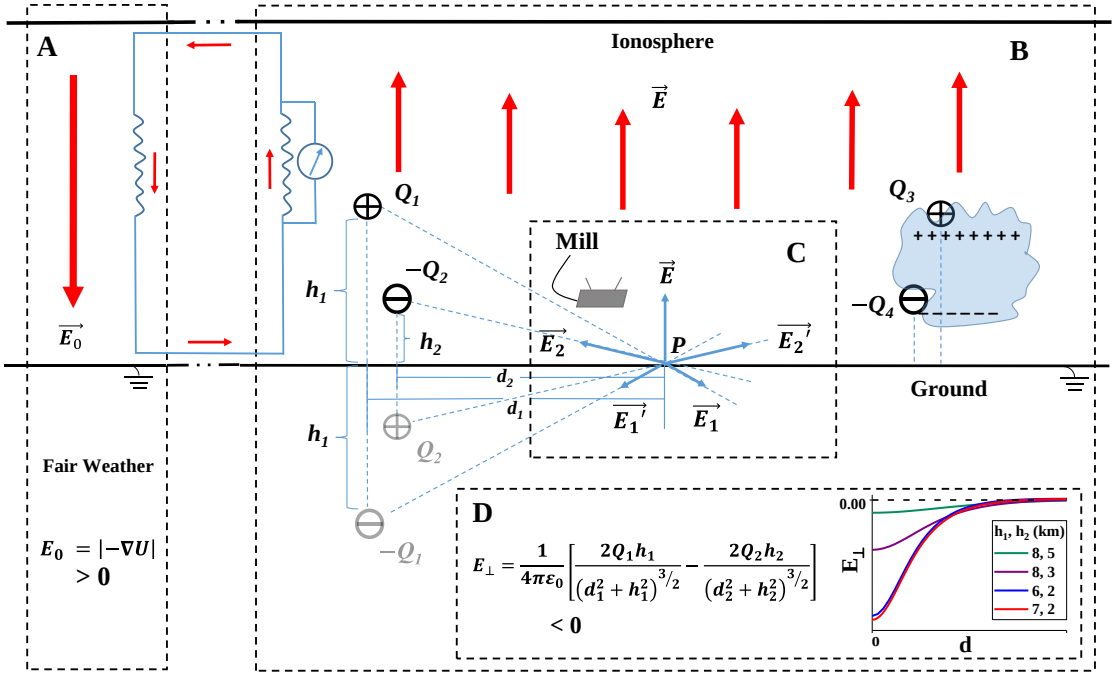

Figure A1: A diagram illustrates the global electric circuit. Part A: The atmospheric electric field under fair weather with a downward field returning from the ionosphere. Part B: The dynamo area, with thunderstorms generating an upward electric field towards the ionosphere. The electric field intensity $E_\perp$ could be deduced through the electric imaging method. Part C: The deduced vertical electric field intensity at any point *P* within the thundercloud. Part D: The calculated $E_\perp$ based on the electric imaging method.

Suppose there is positive charge Q_1 at the top of a thunderstorm, with a distance of d_1 above the ground; and a negative charge—Q_2 at the bottom with a distance of d_2. Since the ground surface could be regarded as an infinite conducting plane, it would generate an induced charge. The boundary conditions here is:

$U = 0$ at z=0

$U \to 0$ at infinity

Under the uniqueness theorem, we can remove the ground surface if we put the postulated image charges of—Q_1 and Q_2 to the corresponding mirror points. Then for an arbitrary point *P* near the boundary, the vertical electric field equals to the following expression according to the Coulomb's law:

$$E_\perp = \frac{1}{4\pi\varepsilon_0}\left[\frac{2Q_1h_1}{(d_1^2+h_1^2)^{3/2}} - \frac{2Q_2h_2}{(d_2^2+h_2^2)^{3/2}}\right]. \qquad \text{(A1) (Griffiths, 1999)}$$

In the simplest case, when Q_1 equals to Q_2 and $d_1=d_2=d$, $\boldsymbol{E}_\perp$ varies with the distance *d*. If Q_2 is larger than Q_1 ($Q_2 > Q_1 > 0$), and the negative charge—Q_2 is more closed to the observing point P ($d_2 < d_1$), $\boldsymbol{E}_\perp$ would acquire negative values (e.g., with the upward direction). A brief simulation result is shown by part D, exhibiting a persistent negative values for $\boldsymbol{E}_\perp$.

Data availability

The data sets of sodium fluorescence lidar at Hefei and three kinds of instruments at Wuhan (the ionosonde, electric mill and the fluxgate magnetometer) are publicly available from the Chinese Meridian Project database at http://data.meridianproject.ac.cn/. The access to the sodium density and temperature data by the USTC T/W lidar is referred to National Space Science Data Center, National Science & Technology Infrastructure of China (http://www.nssdc.ac.cn). The lightning location and power data can be downloaded from the World- Wide Lightning Location Network (http://wwlln.net/).

Acknowledgements

This work is supported by the National Natural Science Foundation of China (41974178) and the National Key R&D Program of China (2017YFC0602202). We acknowledge the use of data from the Chinese Meridian Project for the sodium fluorescence lidar at Hefei and three kinds of instruments at Wuhan (the ionosonde, electric mill and the fluxgate magnetometer, http://data.meridianproject.ac.cn/). We thank the World-Wide Lightning Location Network (http://wwlln.net/), a collaboration among over 50 universities and institutions, for providing the lightning location data used in the plotted figures. We also acknowledge the constructive reviews by both referees. The first author would like to thank Chen Hao and Liu Yandong for their help on debugging programs.

Author information

Affiliations

Department of Geophysics, College of the Geology Engineering and Geomatics, Chang'an University, Xi'an, 710054, China

Shican Qiu & Ning Wang,

Key Laboratory of Geospace Environment, Chinese Academy of Sciences, University of Science & Technology of China, Hefei, Anhui, 230026

Shican Qiu, Gaopeng Lu, Mingjiao Jia, Xianghui Xue, Tao li & Xiankang Dou

Mengcheng National Geophysical Observatory, School of Earth and Space Sciences, University of Science and Technology of China, Hefei, Anhui, 230026, China

Mingjiao Jia, Xianghui Xue, Tao li & Xiankang Dou

Gravity & Magnetic Institute of Chang'an University, Xi'an, 710054, China

Ning Wang

Key Laboratory of Western China's Mineral Resources and Geological Engineering, China Ministry of Education, Xi'an, 710054, China

Ning Wang

Center for Environmental Research and Earth Sciences (CERES), Salem, Massachusetts, 01970, USA

Willie Soon

Contributions

Shican Qiu conceived this study and wrote this manuscript. She also prepared Fig. 2~5 in the main text and Fig. A1 in the Appendix.

Ning Wang performed data analysis.

Willie Soon was in charge of the organization and English polishing of the whole manuscript.

Gaopeng Lu added some materials about thunderstorms and lightning strokes.

Mingjiao Jia prepared Fig. 1 and gave some useful comments on the content.

Xianghui Xue wrote the response to reviewers and added some materials in the discussion.

Tao Li helped with the response to reviewers.

Xiankang Dou conceived this study and provided data from the Chinese Meridian Project.

Competing interests

The authors declare no conflict of interest.

References

Abdu, M. A., Macdougall, J. W., Batista, I. S., Sobral, J. H. A., and Jayachandran, P. T.: Equatorial evening prereversal electric field enhancement and sporadic E layer disruption: A manifestation of E and F region coupling, Journal of Geophysical Research Space Physics, 108, SIA 8-1-SIA 8-13, 2003.

Beatty, T. J., Collins, R. L., Gardner, C. S., Hostetler, C. A., Sechrist, C. F., and Tepley, C. A.: Simultaneous radar and lidar observations of sporadic E and Na layers at Arecibo, Geophysical Research Letters, 16, 1019-1022, 1989.

Bittencourt, J. A.: Fundamentals of Plasma Physics, 3rd ed., Springer-Verlag New York, Inc, 9-10pp, 2004.

Bortnik, J., Thorne, R. M., O'Brien, T. P., Green, J. C., Strangeway, R. J., Shprits, Y. Y., and Baker, D. N.: Observation of two distinct, rapid loss mechanisms during the 20 November 2003 radiation belt dropout event, Journal of Geophysical Research: Space Physics, 111, A12216, 2006.

Chimonas, G., and Axford, W. I.: Vertical movement of temperate-zone sporadic E layers, Journal of Geophysical Research, 73, 111-117, 1968.

Christos, H.: Is there a conclusive evidence on lightning-related effects on sporadic E layers?, Journal of Atmospheric and Solar-Terrestrial Physics, 172, 117-121, 2018.

Clemesha, B. R, Kirchhoff, V., Simonich, D.W., and Takahashi, H.: Evidence of an extra-terrestrial source for the mesospheric sodium layer, Geophysical Research Letters, 5, 873-876, 1978.

Clemesha, B. R, Kirchhoff, V., Simonich, D.W., Takahashi, H., and Batista, P.: Spaced lidar and nightglow observations of an atmospheric sodium enhancement, Journal of Geophysical Research: Space Physics, 85, 3480-3484, 1980.

Clemesha, B. R., Simonich, D. M., Batista, P. P., and Batista, I. S.: Lidar observations of atmospheric sodium at an equatorial location, Journal of Atmospheric and Solar-Terrestrial Physics, 60, 1773-1778, 1998.

Clemesha, B. R., Batista, P., and Simonich, D.: An evaluation of the evidence for ion recombination as a source of sporadic neutral layers in the lower thermosphere, Advances in Space Research, 24, 547-556, 1999.

Collins, S. C., Plane, J. M. C., Kelley, M. C., Wright, T. G., Soldán, P., Kane, T. J., Gerrard, A. J., Grime,B. W., Rollason, R. J., and Friedman, J. S., González, S. A., Zhou, Q., Sulzer, M. P., Tepley, C.A.: A study of the role of ion-molecule chemistry in the formation of sporadic sodium layers, Journal of atmospheric and solar-terrestrial physics, 64, 845-860, 2002.

Cox, R., Plane, J. M. C, and Green, J.S.A: A modelling investigation of sudden sodium layers, Geophysical Research Letters, 20, 2841-2844, 1993.

Cox, R. M., and Plane, J. M. C: An ion-molecule mechanism for the formation of neutral sporadic Na layers, Journal of Geophysical Research, 103, 6349-6359, 1998.

Cummer, S. A., Li, J., Han, F., Lu, G., Jaugey, N., Lyons, W. A., and Nelson, T. E.: Quantification of the troposphere-to-ionosphere charge transfer in a gigantic jet, Nature Geoscience, 2, 617-620, 2009.

Curtius, J., Lovejoy, E. R., and Froyd, K. D.: Atmospheric Ion-induced Aerosol Nucleation, Space Science Reviews, 125, 159-167, 2006.

Daire, S. E., Plane, J. M. C, Gamblin, S. D., Soldán, P., Lee, E. P. F, and Wright, T. G.: A theoretical study of the ligand-exchange reactions of $Na^+\cdot$ X complexes (X= O, O_2, N_2, CO_2 and H_2O): implications for the upper atmosphere, Journal of atmospheric and solar-terrestrial physics, 64, 863-870, 2002.

Damtie, B., Nygrén, T., Lehtinen, M. S., and Huuskonen, A.: High resolution observations of sporadic-E layers within the polar cap ionosphere using a new incoherent scatter radar experiment, Annales Geophysicae, 20, 1429-1438, 2003.

Davis, C. J., and Johnson, C. G.: Lightning-induced intensification of the ionospheric sporadic E layer, Nature, 435, 799-801, 2005.

Davis, C. J., and Lo, K. H.: An enhancement of the ionospheric sporadic -E layer in response to negative polarity cloud-to-ground lightning, Geophysical Research Letters, 35, L05815, 2008.

Denardini, C. M., Resende, L. C. A., Moro, J., and Chen, S. S.: Occurrence of the blanketing sporadic E layer during the recovery phase of the October 2003 superstorm, Earth Planets & Space, 68, 1-9, 2016.

Dou, X. K., Xue, X. H., Chen, T. D., Wan, W. X., Cheng, X. W., Li, T., Chen, C., Qiu, S.C. and Chen, Z. Y.: A statistical study of sporadic sodium layer observed by Sodium lidar at Hefei (31.8° N, 117.3° E), Annales Geophysicae, 27, 2247-2257, 2009.

Dou, X. K., Xue, X. H., Li, T., Chen, T. D., Chen, C., and Qiu, S. C.: Possible relations between meteors, enhanced electron density layers, and sporadic sodium layers, Journal of Geophysical Research: Space Physics, 115, A06311, 2010.

Driscoll, K. T., Blakeslee, R. J., and Baginski, M. E.: A modeling study of the time-averaged electric currents in the vicinity of isolated thunderstorms, Journal of Geophysical Research Atmospheres, 97, 11535-11551, 1992.

England, S. L., Maus, S., Immel, T. J., and Mende, S. B.: Longitudinal variation of the E-region electric fields caused by atmospheric tides, Geophysical Research Letters, 33, L21105, 2006.

Fukunishi, H., Takahashi, Y., Kubota, M., Sakanoi, K., Inan, U, S., and Lyons, W. A.: Elves: Lightning-induced transient luminous events in the lower ionosphere, Geophysical Research Letters, 23, 2157-2160, 1996.

Gardner, C. S., Kane, T. J., Senft, D. C., Qian, J., and Papen, G. C.: Simultaneous observations of sporadic E, Na, Fe, and Ca^+ layers at Urbana, Illinois: Three case studies, Journal of Geophysical Research: Atmospheres, 98, 16865-16873, 1993.

Gardner, C. S., Tao, X., and Papen, G. C.: Observations of strong wind shears and temperature enhancements during several sporadic Na layer events above Haleakala, Geophysical Research Letters, 22, 2809-2812, 1995.

Gardner, C. S., Voelz, D., Sechrist Jr, C., and Segal, A.: Lidar studies of the nighttime sodium layer over Urbana, Illinois: 1. Seasonal and nocturnal variations, Journal of Geophysical Research, 91, 13659-13673, 1986.

Girish, T. E., and Eapen, P. E.: Geomagnetic and sunspot activity associations and ionospheric effects of lightning phenomena at Trivandrum near dip equator, Journal of Atmospheric and Solar-Terrestrial Physics, 70, 2222-2232, 2008.

Gong, S. S., Yang, G. T., Wang, J. M., Liu, B. M., Cheng, X. W., Xu, J. Y., and Wan, W. X.: Occurrence and characteristics of sporadic sodium layer observed by lidar at a mid-latitude location, Journal of Atmospheric and Solar-Terrestrial Physics, 64, 1957-1966, 2002.

Gong, S., Zeng, X., Xue, X., Zheng, W., Hu, Z., Jia, H., Zhang, H., and Liu, Y.: First time observation of sodium layer over Wuhan, China by sodium fluorescence lidar, Science in China Series A, 40, 1228-1232, 1997.

Griffiths, D.J.: Introduction to Electrodynamics, 3rd ed., Prentice- Hall, Upper Saddle River, New Jersey, 121-122pp, 1999.

Haldoupis, C., Pancheva, D., and Mitchell, N. J.: A study of tidal and planetary wave periodicities present in midlatitude sporadic E layers, Journal of Geophysical Research, 109, A02302, 2004.

Haldoupis, C., Cohen, M., Cotts, B., Arnone, E., and Inan, U.: Long-lasting D-region ionospheric modifications, caused by intense lightning in association with elve and sprite pairs, Geophysical Research Letters, 39, L16801, 2012.

Harrison, R. G., Aplin, K. L., and Rycroft, M. J.: Atmospheric electricity coupling between earthquake regions and the ionosphere, Journal of Atmospheric & Solar -Terrestrial Physics, 72, 376-381, 2010.

Harrison, R. G.: Behind the curve: a comparison of historical sources for the Carnegie curve of the global atmospheric electric circuit, Hist. Geo Space. Sci., 11, 207-213, 2020.

Hines, C. O.: The Formation of Midlatitude Sporadic E Layers, Journal of Geophysical Research, 69, 1018-1019, 1964.

Immel, T. J., Mende, S. B., Hagan, M. E., Kintner, P. M., and England, S. L.: Evidence of Tropospheric Effects on the Ionosphere, Eos Transactions American Geophysical Union, 90, 69-70, 2013.

Jánský, J., and Pasko, V. P.: Charge balance and ionospheric potential dynamics in time dependent global electric circuit model, Journal of Geophysical Research: Space Physics, 119, 10, 2014.

Johnson, C. G., and Davis, C. J.: The location of lightning affecting the ionospheric sporadic-E layer as evidence for multiple enhancement mechanisms, Geophysical Research Letters, 33, L07811, 2006.

Johnson, M. P., Inan, U. S., Lev-Tov, S. J., and Bell, T. F.: Scattering pattern of lightning-induced ionospheric disturbances associated with early/fast VLF events, Geophysical Research Letters, 26, 2363-2366, 1999.

Kane, T., Grime, B., Franke, S., Kudeki, E., Urbina, J., Kelley, M., and Collins, S.: Joint observations of sodium enhancements and field-aligned ionospheric irregularities, Geophysical Research Letters, 28, 1375-1378, 2001.

Kane, T. J., Hostetler, C. A., and Gardner, C. S.: Horizontal and vertical structure of the major sporadic sodium layer events observed during ALOHA-90, Geophysical Research Letters, 18, 1365-1368, 1991.

Kane, T. J., Gardner, C. S., Zhou, Q., Mathews, J. D., and Tepley, C. A.: Lidar, radar and airglow observations of a prominent sporadic Na/sporadic E layer event at Arecibo during AIDA-89, Journal of Atmospheric & Terrestrial Physics, 55, 499-511, 1993.

Kirkwood, S., and von Zahn, U.: On the role of auroral electric fields in the formation of low altitude sporadic-E and sudden sodium layers, Journal of Atmospheric & Terrestrial Physics, 53, 389-407, 1991.

Kirkwood, S., and Nilsson, H.: High-latitude Sporadic-E and other Thin Layers – the Role of Magnetospheric Electric Fields, Space science Reviews, 91, 579-613, 2000.

Kumar, V. V., Parkinson, M. L., Dyson, P. L., and Burns, G. B.: The effects of thunderstorm-generated atmospheric gravity waves on mid-latitude F-region drifts, Journal of Atmospheric and Solar-Terrestrial Physics, 71, 1904-1915, 2009.

Kuo, C. L., and Lee, L. C.: Ionospheric plasma dynamics and instability caused by upward currents above thunderstorms, Journal of Geophysical Research: Space Physics, 120, 3240-3253, 2015.

Kwon, K. H., Senft, D. C., and Gardner, C. S.: Lidar observations of sporadic sodium layers at Mauna Kea Observatory, Hawaii, Journal of Geophysical Research Atmospheres, 93, 14199-14208, 1988.

Lay, E. H., Shao, X. M., Kendrick, A. K., and Carrano, C. S.: Ionospheric acoustic and gravity waves associated with midlatitude thunderstorms, Journal of Geophysical Research Space Physics, 120, 6010-6020, 2015.

Leblanc, F., Aplin, K. L., Yair, Y., Harrison, R. G., Lebreton, J. P., and Blanc, M.: Planetary Atmospheric Electricity, 2008.

Li, T., Fang, X., Liu, W., Gu, S. Y., and Dou, X.K.: Narrowband sodium lidar for the measurements of mesopause region temperature and wind, Applied Optics, 51, 5401-5411, 2012.

Lv, D. R., Fan, Y., and Xu, J. Y.: Advances in Studies of the Middle and Upper Atmosphere and Their Coupling with the Lower Atmosphere, Advances in Atmospheric sciences, 21, 361-368, 2004.

Macdougall, J. W., and Jayachandran, P. T.: Sporadic E at cusp latitudes, Journal of Atmospheric and Solar-Terrestrial Physics, 67, 1419-1426, 2005.

Mangla, B., Sharma, D. K., and Rajput, A.: Ion density variation at upper ionosphere during thunderstorm, Advances in Space Research, 59, 1189-1199, 2016.

Marsh, D. R., Janches, D., Feng, W., and Plane, J. M. C.: A global model of meteoric sodium, Journal of Geophysical Research: Atmospheres, 118, 11442-11452, 2013.

Maruyama, T.: Extreme enhancement in total electron content after sunset on 8 November 2004 and its connection with storm enhanced density, Geophysical Research Letters, 33, L20111, 2006.

Mathews, J. D., Zhou, Q., Philbrick, C. R., Morton, Y. T., and Gardner, C. S.: Observations of ion and sodium layer coupled processes during AIDA, Journal of Atmospheric & Terrestrial Physics, 55, 487-498, 1993.

Mathews, J. D.: Sporadic E: current views and recent progress, Journal of Atmospheric and Solar-Terrestrial Physics, 60, 413-435, 1998.

Matuura, N., Tsuda, T., and Nozawa, S.: Field-aligned current loop model on formation of sporadic metal layers, Journal of Geophysical Research: Space Physics, 118, 4628-4639, 2013.

Miyagawa, H., Nakamura, T., Tsuda, T., Abo, M., Nagasawa, C., Kawahara, T. D., Kobayashi, K., Kitahara, T., Nomura, A.: Observations of mesospheric sporadic sodium layers with the MU radar and sodium lidars, Earth Planets & Space, 51, 785-797, 1999.

Nagasawa, C., and Abo, M.: Lidar observations of a lot of sporadic sodium layers in mid-latitude, Geophysical Research Letters, 22, 263-266, 1995.

Nesse, H., Heinrich, D., Williams, B., Hoppe, U. P., Stadsnes, J., Rietveld, M., Singer, W., Blum, U., Sandanger, M. I., and Trondsen, E.: A case study of a sporadic sodium layer observed by the ALOMAR Weber Na lidar, Annales Geophysicae, 26, 1071-1081, 2008.

Nygrén, T., Aikio, A. T., Voiculescu, M., and Ruohoniemi, J. M.: IMF effect on sporadic-E layers at two northern polar cap sites: Part II – Electric field, Annales Geophysicae, 24, 901-913, 2006.

Plane, J. M. C., Cox, R. M., and Rollason, R. J.: Metallic layers in the mesopause and lower thermosphere region, Advances in Space Research, 24, 1559-1570, 1999.

Plane, J. M. C.: Atmospheric chemistry of meteoric metals, Chemical Reviews, 103, 4963-4984, 2003.

Parkinson, M. L., Dyson, P. L., Monselesan, D. P., and Morris, R. J.: On the role of electric field direction in the formation of sporadic E-layers in the southern polar cap ionosphere, Journal of Atmospheric and Solar-Terrestrial Physics, 60, 471-491, 1998.

Pasko, V. P., Stanley, M. A., Mathews, J. D., Inan, U. S., and Wood, T. G.: Electrical discharge from a thundercloud top to the lower ionosphere, Nature, 416, 152-154, 2002.

Pasko, V. P.: Blue jets and gigantic jets: transient luminous events between thunderstorm tops and the lower ionosphere, Plasma Physics & Controlled Fusion, 50, 124050, 2008.

Qiu, S. C, Tang, Y. H, and Dou, X. K: Temperature controlled icy dust reservoir of sodium: A possible mechanism for the formation of sporadic sodium layers, Advances in Space Research, 55, 2543-2565, 2015.

Qiu, S. C, Tang, Y. H, Jia, M. J, Xue, X. H, Dou, X. K, Li, T., and Wang, Y. H: A review of latitudinal characteristics of sporadic sodium layers, including new results from the Chinese Meridian Project, Earth-Science Reviews, 162, 83-106, 2016.

Resende, L. C. A., and Denardini, C. M.: Equatorial sporadic E-layer abnormal density enhancement during the recovery phase of the December 2006 magnetic storm: A case study, Earth Planets & Space, 64, 345-351, 2012.

Resende, L. C. A., Denardini, C. M., and Batista, I. S.: Abnormal fbEs enhancements in equatorial Es layers during magnetic storms of solar cycle 23, Journal of Atmospheric and Solar-terrestrial Physics, 102, 228-234, 2013.

Roble, R. G., and Hays, P. B.: A Quasi-static model of global atmospheric electricity 2. Electrical coupling between the upper and lower atmosphere, Journal of geophysical research, 84, 7247-7256, 1979.

Rodger, C. J., Cho, M., Clilverd, M. A., and Rycroft, M. J.: Lower ionospheric modification by lightning-EMP: Simulation of the night ionosphere over the United States, Geophysical Research Letters, 28, 199-202, 2001.

Rycroft, M. J., Israelsson, S., and Price, C.: The global atmospheric electric circuit, solar activity and climate change, Journal of Atmospheric & Solar Terrestrial Physics, 62, 1563-1576, 2000.

Rycroft, M. J.: Electrical processes coupling the atmosphere and ionosphere: An overview, Journal of Atmospheric and Solar-Terrestrial Physics, 68, 445-456, 2006.

Rycroft, M. J., Odzimek, A., Arnold, N. F., Füllekrug, M., Kulak, A., and Neubert, T.: New model simulations of the global atmospheric electric circuit driven by thunderstorms and electrified shower clouds: The roles of lightning and sprites, Journal of Atmospheric & Solar Terrestrial Physics, 69, 2485-2509, 2007.

Rycroft, M. J., and Harrison, R. G.: Electromagnetic Atmosphere-Plasma Coupling: The Global Atmospheric Electric Circuit, Space Sci Rev, 168, 363–384, 2012.

Rycroft, M. J., Nicoll, K. A., Aplin, K. L., and Harrison, R.G.: Recent advances in global electric circuit coupling between the space environment and the troposphere, Journal of Atmospheric and Solar-Terrestrial Physics, 90-91, 198-211, 2012.

Sátori, G., Rycroft, M. J, Bencze, P., Märcz, F., Bór, J., Barta, V., Nagy, T., and Kovács, K.: An Overview of Thunderstorm-Related Research on the Atmospheric Electric Field, Schumann Resonances, Sprites, and the Ionosphere at Sopron, Hungary, Surveys in Geophysics, 34, 255-292, 2013.

Šauli, P., and Bourdillon, A.: Height and critical frequency variations of the sporadic-E layer at mid-latitudes, Journal of Atmospheric and Solar-Terrestrial Physics, 70, 1904-1910, 2008.

Sentman, D. D., and Wescott, E. M.: Red sprites and blue jets: Thunderstorm-excited optical emissions in the stratosphere, mesosphere, and ionosphere, Physics of Plasmas, 2, 2514-2522, 1995.

Seyler, C. E., Rosado-Román, J. M., and Farley, D. T.: A nonlocal theory of the gradient-drift instability in the ionospheric E-region plasma at mid-latitudes, Journal of Atmospheric and Solar-Terrestrial Physics, 66, 1627-1637, 2004.

Shao, X. M., Lay, E. H., and Jacobson, A. R.: Reduction of electron density in the night-time lower ionosphere in response to a thunderstorm, Nature Geoscience, 6, 29-33, 2013.

Sharma, D. K., Rai, J., Israil, M., Subrahmanyam, P., Chopra, P., and Garg, S. C.: Enhancement in ionospheric temperatures during thunderstorms, Journal of Atmospheric and Solar-Terrestrial Physics, 66, 51-56, 2004.

Shibata, Y., Nagasawa, C., Abo, M., Maruyama, T., Saito, S., and Nakamura, T.: Lidar Observations of Sporadic Fe and Na Layers in the Mesopause Region over Equator, Journal of the Meteorological Society of Japan, 84A, 317-325, 2006.

Somov, B. V.: Cosmic Plasma Physics, Springer Science+Business Media Dordrecht, 2000.

Su, H. T., Hsu, R. R., Chen, A. B., Wang, Y. C., Hsiao, W. S., Lai, W. C., Lee, L. C., Sato, M., and Fukunishi, H.: Gigantic jets between a thundercloud and the ionosphere, Nature, 423, 974-976, 2003.

Suparta, W., and Fraser, G. J.: A New Method to Correlate a Possible Coupling between the Upper and the Lower Atmosphere, American Journal of Applied sciences, 9, 894-901, 2012.

Surkov, V. V., Hayakawa, M., Schekotov, A. Y., Fedorov, E. N., and Molchanov, O. A.: Ionospheric Alfvén resonator excitation due to nearby thunderstorms, Journal of Geophysical Research, 111, A01303, 2006.

Takahashi, T., Nozawa, S., Tsuda, T.T., Ogawa, Y., Saito, N., Hidemori, T., Kawahara, T. D., Hall, C., Fujiwara, H., Matuura, N., Brekke, A., Tsutsumi, M., Wada, S., Kawabata, T., Oyama, S., and Fuji, R.: A case study on generation mechanisms of a sporadic sodium layer above Tromso (69.6 degrees N) during a night of high auroral activity, Annales Geophysicae, 33, 941-953, 2015.

Tinsley, B. A.: Influence of Solar Wind on the Global Electric Circuit, and Inferred Effects on Cloud Microphysics, Temperature, and Dynamics in the Troposphere, Space Science Reviews, 94, 231-258, 2000.

Voiculescu, M., Aikio, A. T., Nygrén, T., and Ruohoniemi, J. M.: IMF effect on sporadic-E layers at two northern polar cap sites: Part I - Statistical study, Annales Geophysicae, 24, 887-900, 2006.

von Zahn, U., von der Gathen, P., and Hansen, G.: Forced release of sodium from upper atmospheric dust particles, Geophysical Research Letters, 14, 76-79, 1987.

von Zahn, U., Goldberg, R., Stegman, J., and Witt, G.: Double-peaked sodium layers at high latitudes, Planetary and space science, 37, 657-667, 1989.

Wakabayashi, M., and Ono, T.: Multi-layer structure of mid-latitude sporadic-E observed during the SEEK-2 campaign, Annales Geophysicae, 23, 2347-2355, 2005.

Wan, W., Liu, L., Parkinson, M. L., Liu, R., He, L., Breed, A. M., Dyson, P. L., and Morris, R. J.: The effect of fluctuating ionospheric electric fields on Es-occurrence at cusp and polar cap latitudes, Advances in Space Research, 27, 1283-1288, 2001.

Wang, C.: New Chains of Space Weather Monitoring Stations in China, Space Weather, 8, S08001, 2010.

Wilkinson, P. J., Szuszczewicz, E. P., and Roble, R. G.: Measurements and modelling of intermediate, descending, and sporadic layers in the lower ionosphere: Results and implications for global-scale ionospheric-thermospheric studies, Geophysical Research Letters, 19, 95-98, 1992.

Williams, B. P., Croskey, C. L., She, C. Y., Mitchell, J. D., and Goldberg, R. A.: Sporadic sodium and E layers observed during the summer 2002 MaCWAVE/MIDAS rocket campaign, Annales Geophysicae, 24, 1257-1266, 2006.

Yu, B., Xue, X., Lu, G., Ma, M., Dou, X., Qie, X., Ning, B., Hu, L. H., Wu, J., and Chi, Y.: Evidence for lightning-associated enhancement of the ionospheric sporadic E layer dependent on lightning stroke energy, Journal of Geophysical Research Space Physics, 120, 9202-9212, 2015.

Yu, B., Xue, X., Lu, G., Kuo, C. L., Dou, X., Gao, Q., Qie, X., Wu, J., Qiu, S. C, and Chi, Y.: The enhancement of neutral metal Na layer above thunderstorms, Geophysical Research Letters, 44, 9555-9563, 2017.

Zhang, L., Tinsley, B., and Zhou, L.: Low Latitude Lightning Activity Responses to Cosmic Ray Forbush Decreases, Geophysical Research Letters, 47, e2020GL087024, 2020.

Zhang, Y., Wu, J., Guo, L., Hu, Y., Zhao, H., and Xu, T.: Influence of solar and geomagnetic activity on sporadic-E layer over low, mid and high latitude stations, Advances in Space Research, 55, 1366-1371, 2015.

Zhou, Q., Mathews, J. D., and Tepley, C. A.: A proposed temperature dependent mechanism for the formation of sporadic sodium layers, Journal of Atmospheric and Terrestrial Physics, 55, 513-521, 1993.

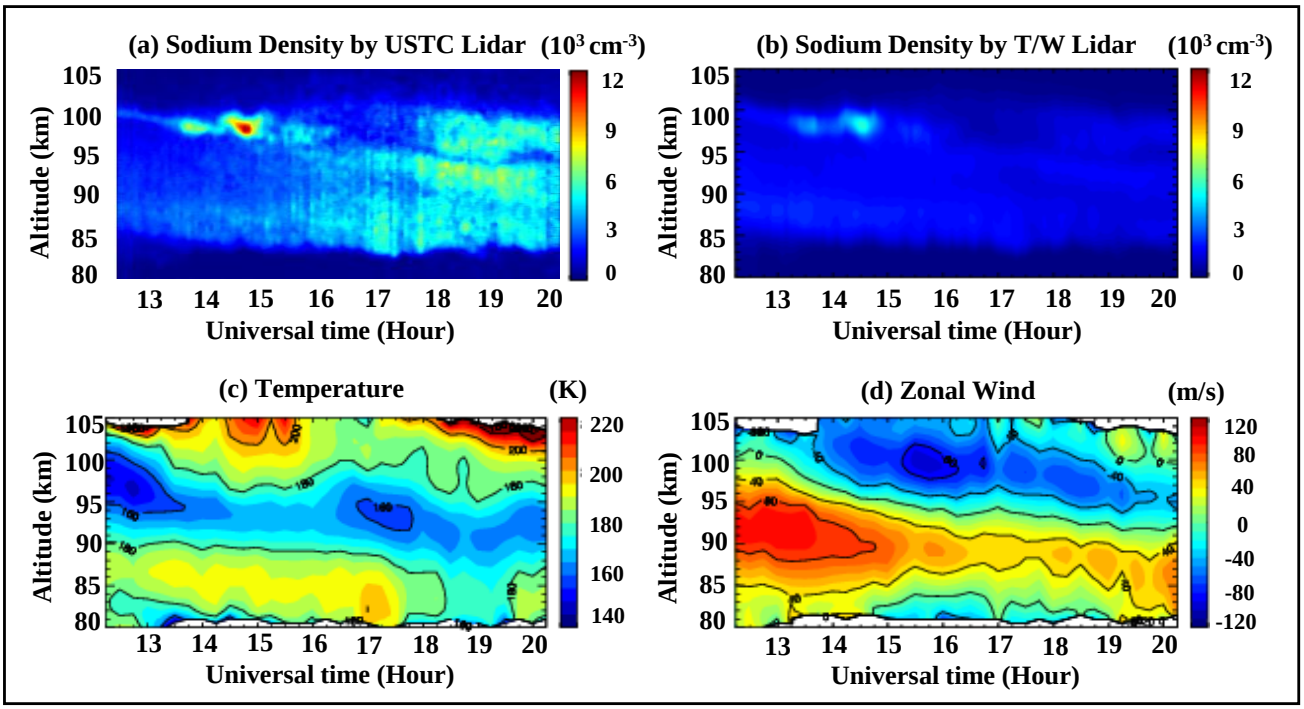

Figure 1: Observations on June 3rd, 2013, by the USTC sodium lidar and T/W lidar. (a) The sodium density detected by the USTC lidar. A moderate increase of sodium density appears at about 13:20 UT, while the largest intensity of sodium enhancement begins at about 14:20 UT. The sodium density peaks at 14:40 UT around 97.75 km. (b) The sodium density profile by T/W lidar, with a different resolution. (c) Temperature profile observed by the nearby T/W lidar, showing a cold region where the Nas occurs. (d) The zonal wind detected by the T/W lidar, exhibiting a suitable wind shear for the creation or formation of Es.

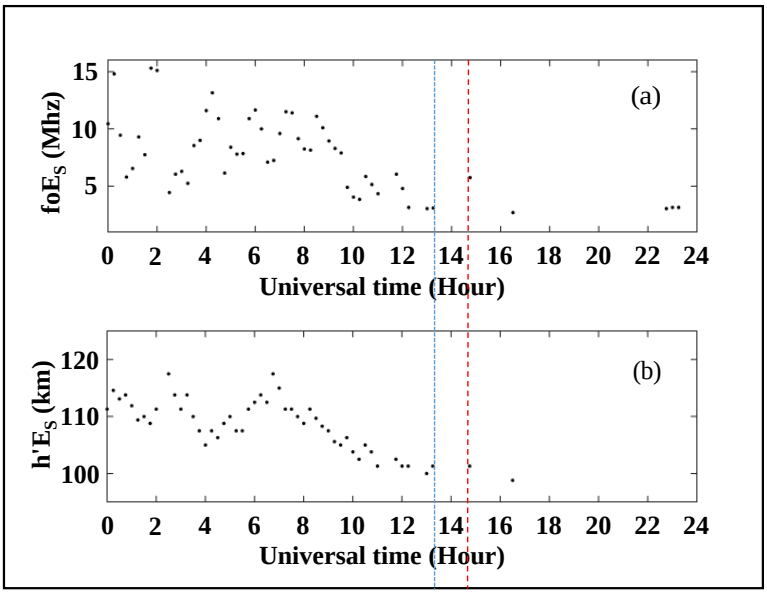

Figure 2: Sporadic E layers observed by the ionosonde at Wuhan (30.5°N，114.6°E). (a) The time series of the critical frequency for E_S (foE_S). The E_S layers travel/propagate downward starting around 6:30 UT, and deplete altogether at about 13:20 UT. (b) The visual height of E_S ($h'E_S$). The vertical blue dotted line annotates the beginning of the Na_S around 13:20 UT, and the vertical red dashed line points out the time when the most intense sodium enhancement starts on 14:20 UT.

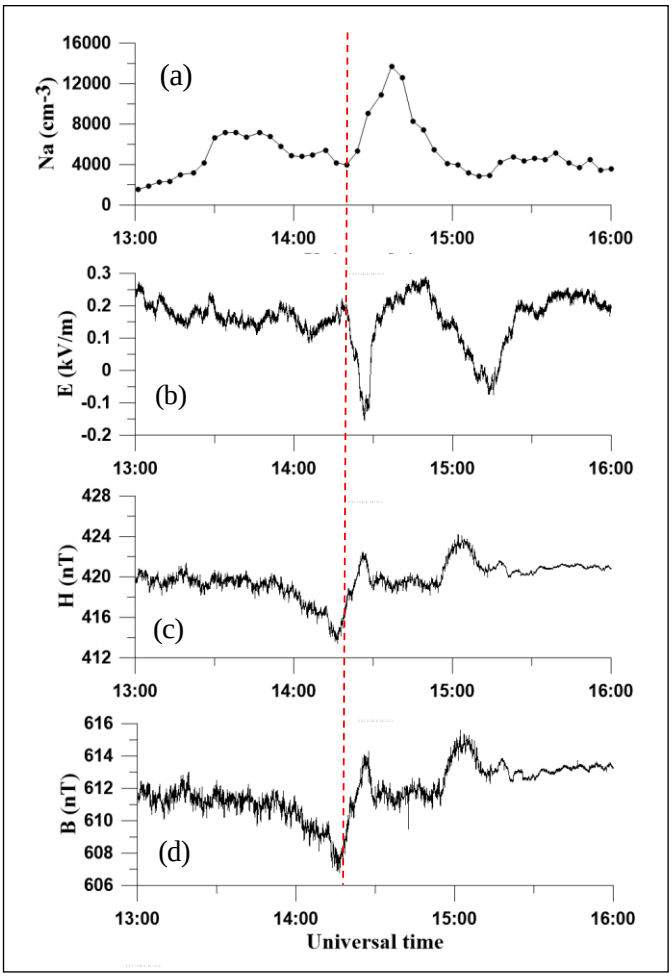

Figure 3: Observations of some atmospheric parameters and some deduced results. (a) Time series of sodium density variations at peak height 97.75 km. The sodium density begins to increase at about 14:20 UT. (b) Atmospheric electric field variations, exhibiting a synchronous overturning from 14:20 UT with the enhancement of sodium density (also pointed out by the vertical red dashed line). Note that there is another overturning peaking at 15:15 UT, without another Na_S being produced, which could be explained by a depletion of ions in the E_S. The electric field recovers at about 15:30 UT. (c) Horizontal magnetic field observed by the fluxgate magnetometer. (d) The deduced magnetic induction intensity from observations of (*H*, *D*, *Z*) components by the fluxgate magnetometer ($B = \sqrt{H^2 + D^2 + Z^2}$).

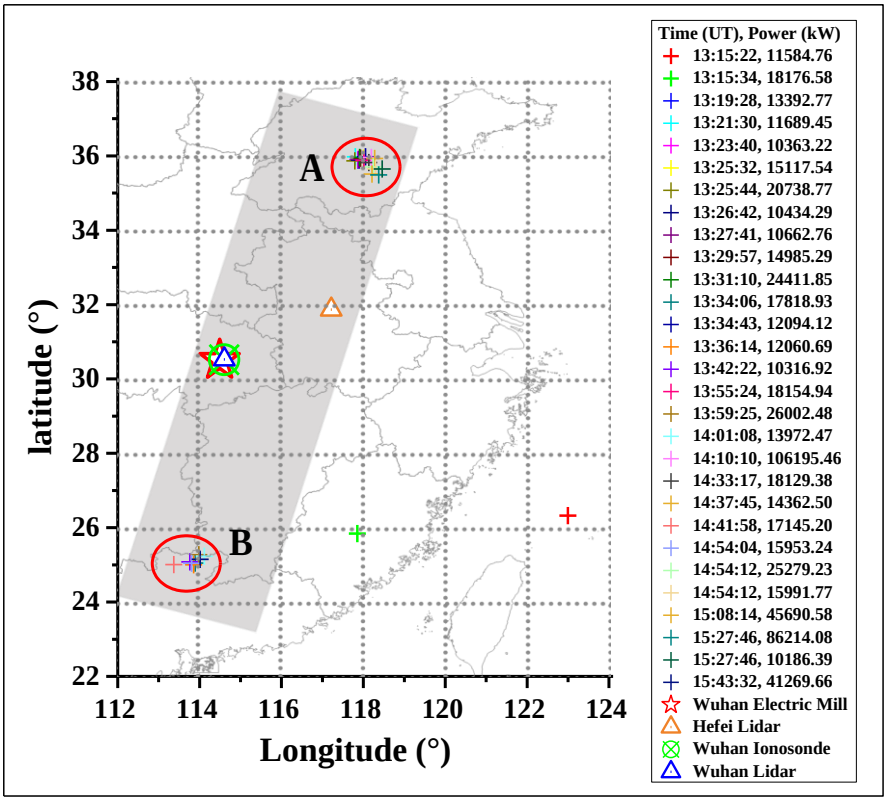

Figure 4: The lightning strokes are detected by WWLLN. The continuous strongest lightnings with a power larger than 10^4 kW occur from 13:19 UT to 15:43 UT, mainly concentrating around areas within (35.8°N, 118.1°E) and (25.1°N, 113.8°E), respectively.

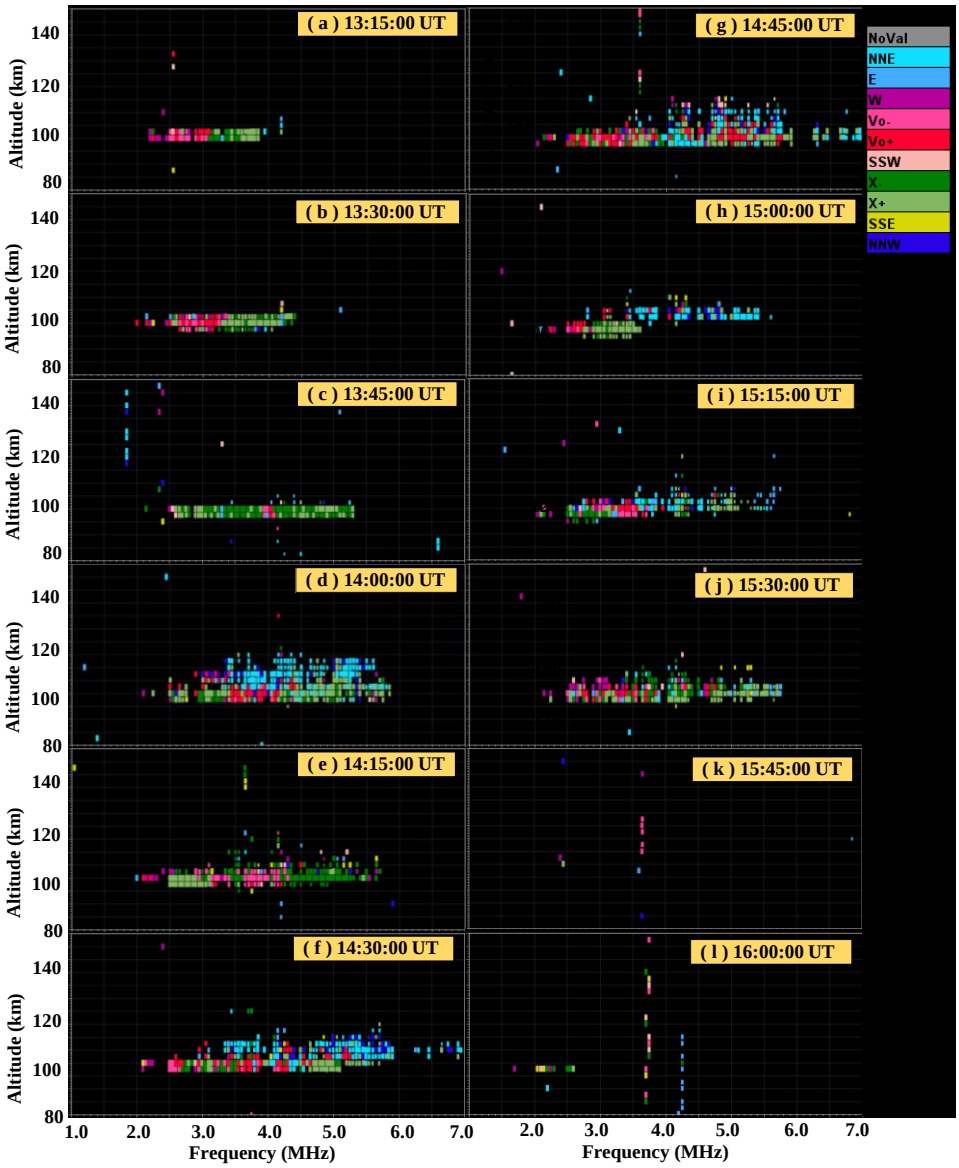

Figure 5: Extraordinary echoes by Wuhan ionosonde in different modes: (a) ~ (c): From 13:15 UT to 13:45 UT, the echoes gradually increase. Note that the powerful lightning period begins on 13:15 UT as well, with the sodium density enhancement and the E_S depletion occurring on about 13:20 UT. (d) ~ (g): Most intense echo signals occur during 14:00 UT to 14:45 UT, while the largest intensity of sodium enhancement begins at 14:20 UT and the sodium density peaks at 14:40 UT. The overturning of electric field also occurs at 14:20 UT. (h) ~ (j): From 15:00 UT to 15:30 UT, the signals weaken gradually. (k) ~ (l): The echoes vanish after 15:45 UT. Afterwards, no strong stroke detected again within the discussed area. Meanwhile, the ionospheric echoes diminish after 15:45 UT, and the overturning of electric field also recovers at about 15:30 UT.

Table 1 : The nature of foE$_S$ variations under the situations of the overturning of electric field

foE$_S$ Variations	Termination	Decrease	Generation	Increase	Others
Ratios (Case days/Total days)	155/242	39/242	6/242	26/242	28/242